Landslide Prediction via Multispectral Satellite Imagery: A Multi-Band Convolutional Neural Network Approach

Chethana Vasudevaiah
B.M.S. College of Engineering, Bull Temple Road, Bengaluru -560019, Karnataka, India | Dayananda Sagar College of Engineering, Bangalore-560111, Karnataka, India | Visvesvaraya Technological University, Belagavi-590018, Karnataka, India
chethanav499@gmail.com (corresponding author)

Rashmi Shivaswamy
School of Computer Science and Engineering, RV University, Bangalore-560059, Karnataka, India
rashmineha.s@gmail.com

Rajeshwari Janthakal
Department of Information Science and Engineering, Dayananda Sagar College of Engineering, Bangalore-560111, Karnataka, India | Visvesvaraya Technological University, Belagavi-590018, Karnataka, India
rajeshwarij-ise@dayanandasagar.edu

Received: 21 November 2025 | Revised: 21 December 2025 and 12 January 2026 | Accepted: 14 January 2026

 DOI: https://doi.org/10.48084/etasr.16431

ABSTRACT

Sliding of land of a particular location due to heavy rain, vegetation change, or deforestation is a landslide. The landslides lead to loss of life, damage to infrastructure, and disruption of economic conditions. With the advancement of remote sensing technology, multispectral satellite images are available with various bands. These bands are highly useful for predicting landslides in advance. Along with these bands from satellite images, environmental features, such as rainfall, temperature, soil moisture, and topographical features, such as elevation, slope, aspect, and curvature, provide additional information for prediction. With these layers of information, satellite images of landslide and non-landslide locations in India were trained and tested using a Convolutional Neural Network (CNN) model. The CNN model was built by choosing 3 bands, 5 bands, 10 bands, and 16 bands of satellite images, resulting in prediction accuracies of 67.97%, 73.51%, 78.03%, and 79.47%, respectively. The model performance was assessed using metrics such as accuracy, precision, recall, F1-score, and confusion matrices. The results suggest that selecting a higher number of features leads to higher accuracy. The need for such models in countries like India, where landslides frequently occur, is highlighted. This study demonstrates that integrating topographical and environmental data significantly improves the accuracy of the prediction model.

Keywords-multispectral satellite images; Landslide; Non-landslide; convolutional neural network; prediction

I. INTRODUCTION

In India, landslides frequently occur due to diverse topographical features, including the Western Ghats, the Himalayas, and vast river basin areas. These events result in the loss of human and animal lives and economic damage. The region experiences daily changes caused by deforestation, population growth, and fluctuations in rainfall, temperature, and topography, making landslides unpredictable. Predictive models for landslides are crucial for disaster risk management and emergency planning. Traditional methods depend on geological surveys and historical records, which are often tedious, spatially restricted, and time-intensive. Assessing high-resolution satellite imagery, such as Landsat, Sentinel, and others, through reliable sources, including NASA, USGS, and ISRO, has become easy and economical. Satellites like Landsat provide images with various bands, including Bands 1-11, visible light bands, such as Red, Green, and Blue, and a few other bands, such as NIR, SWIR-1, and SWIR-2. Along with satellite images, topographical features, including elevation, slope, aspect, and curvature, are available with the Digital Elevation Model (DEM) from the USGS. Some bands, like NDVI, NDBI, and NDWI, were generated using the available bands from satellite images. With these available resources,

developing a predictive model using artificial intelligence may help save lives and enable preventive measures before landslides occur. With the present technology, machine learning and deep learning models are more effective for prediction tasks. As the satellite images are available in the form of TIFF files, the present study employed a deep learning model, namely a CNN model, for landslide prediction.

Landslides remain one of the most destructive hydro-geomorphological hazards, particularly in regions with complex terrain, high rainfall variability, and dynamic land-use patterns such as India. Accurate prediction and susceptibility mapping are essential for mitigating loss of life, infrastructure, and the environment. With advancements in remote sensing, machine learning, and deep learning, researchers have focused on integrating spectral, environmental, and topographic information to improve landslide modeling and detection.

Early studies demonstrated the potential of CNNs for large-scale landslide detection using optical satellite imagery, supported by datasets such as the NASA Global Landslide Catalog [1]. Building on these efforts, the fusion of multispectral imagery with terrain attributes (e.g., slope, elevation, aspect), vegetation indices, and deformation signals derived from SAR and DInSAR products was explored. For example, integrating NDVI, DEM-based slopes, and optical bands significantly enhanced susceptibility mapping and object-level detection performance [2]. Deep architectures such as U-Net further improved pixel-level segmentation accuracy by leveraging multiscale feature extraction, especially when applied to rainfall-driven landslides in southern India [3].

Beyond purely CNN-based approaches, hybrid models have gained popularity. Combining CNN feature extraction with machine learning algorithms such as Random Forests has shown improved predictive capability for landslide occurrence [4]. Temporal sequences via CNN–LSTM hybrids have been incorporated to capture rainfall and soil moisture dynamics, yielding improved temporal prediction performance. Graph-based architectures, like SGCN-LSTM, have further extended this concept by enabling real-time landslide monitoring from streaming environmental data [5–7].

Ensemble learning methods are also widely used for susceptibility assessment. Random Forests, XGBoost, and fuzzy inference-based models have been successfully applied using environmental variables such as rainfall, elevation, seismic activity, and soil moisture [8]. The effectiveness of incorporating multispectral indices (NDVI, NDBI, NDWI), SAR-derived deformation, and vegetation stress indicators to improve classification accuracy in landslide-prone regions has been highlighted [9-12]. Advanced deep learning architectures—including enhanced U-Nets, DeepLabV3+, and U-Net variants with residual blocks or attention mechanisms—have shown notable improvements in segmentation and susceptibility mapping when combined with multisource spatial and topographic features. Transformer-based models and Vision Transformers (ViTs) have demonstrated superior contextual modeling and generalization over traditional CNNs, particularly when applied to satellite-image-based disaster prediction [13-15]. Authors in [16] employed CNNs and LSTM, and combined model results with more accuracy.

II. METHODOLOGY

This study utilized 1558 landslide images and 875 non-landslide images for India. These Landsat satellite images were collected from Google Earth Engine data catalog [17], with data locations accessed from NASA landslide data [18]. The image dataset was used to design a CNN with three convolutional blocks followed by fully connected layers. The network processes image inputs of size 64 × 64 pixels with multiple spectral bands. The CNN architecture is illustrated in Figure 1, and its main components are:

A. Input Layer

The input to the CNN consists of image patches of dimension ($64 \times 64 \times B$), where B represents the number of spectral bands.

B. Convolutional Blocks

- First Block (B1): The B1 block includes a 2D convolutional layer with 32 filters of size 3×3, which extracts low-level spatial features (e.g., edges and textures). Feature extraction is followed by a 2×2 max pooling operation to reduce spatial resolution and computational complexity. Batch Normalization is applied to stabilize training.
- Second Block (B2): B2 is a convolutional layer with 64 filters (3×3) and captures additional abstract mid-level features such as shapes and patterns. mid-level feature extraction is again followed by max pooling and batch normalization.
- Third Block (B3): B3 is a convolutional layer with 128 filters (3×3), and it extracts higher-level, complex spatial features, also followed by pooling and normalization.

These three blocks progressively learn hierarchical representations of the input imagery from fine details to abstract contextual features.

C. Flattening Layer

The feature maps generated by the convolutional layers are flattened into a one-dimensional vector, serving as input for the dense layers.

D. Fully Connected Layers

A dense (fully connected) layer with 256 neurons and ReLU activation integrates the extracted features for classification. A dropout layer with a rate of 0.5 is employed to prevent overfitting by randomly deactivating neurons during training.

E. Output Layer

The final dense layer consists of 2 neurons with a SoftMax activation function, producing probability distributions over the two classes: landslide and non-landslide.

F. Training Strategy

The model is compiled using the Adam optimizer with categorical cross-entropy loss, suitable for multi-class classification (two classes in this case). Model performance is evaluated using accuracy as the primary metric.

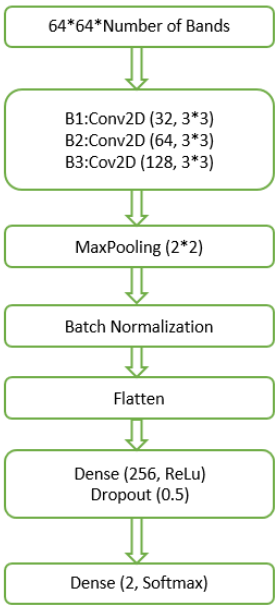

Fig. 1. CNN architecture.

III. RESULTS AND DISCUSSION

The CNN-based landslide prediction model was evaluated under different spectral configurations to assess the impact of input band selection on classification performance. The study compares four configurations using: (i) only Bands 1–3, (ii) Bands 1–3 and 13–16, (iii) Bands 1–3, 7–9, and 13–16, (iv) all available spectral bands (Bands 1–16). Performance was measured in terms of accuracy, precision, recall, F1-score, and confusion matrices.

A. Performance with Bands 1–3 (3 Bands Only)

When trained with only Bands 1–3, with features Red, Green, and Blue, the model achieved a test accuracy of 67.97%. As shown in Figure 2, the landslide prediction accuracy was 0.68. The confusion matrix for Bands 1–3 is depicted in Figure 3(a). The model correctly classified most landslide pixels with a recall of 0.96, but misclassified a large proportion of non-landslide samples, with a recall of 0.17. This imbalance resulted in a high number of false positives (145 cases), where stable terrain was incorrectly predicted as landslides. The corresponding F1-score for the landslide class (0.79) was significantly higher than for the non-landslide class (0.28), indicating that the model was biased toward landslide prediction. As illustrated in Figure 2, weighted average precision, recall, and F1-score for Bands 1–3 were 0.70, 0.68, and 0.61, respectively.

B. Performance with Bands 1–3 and 13-16 (7 Bands Only)

On training sets, 7 selected bands (Bands 1–3 and 13-16) outperform Bands 1–3 with an accuracy of 73.51%. As demonstrated in Figure 2, the landslide prediction accuracy was 0.74. The confusion matrices presented in Figure 3(b) illustrate model performance using Bands 1-3, RGB, and topographical features, such as elevation, slope, aspect, and curvature. In Bands 1–3 and 13-16, the landslide pixels were correctly classified as landslide pixels, with a recall value of 0.87, while the non-landslide pixels were classified with a recall value of 0.49. This shows a classification imbalance with 89 cases of false positives. The landslide class had an F1-score of 0.81, compared to the non-landslide class, which had an F1-score of 0.57. As observed in Figure 2, weighted average precision, recall, and F1-score for Bands 1–3 and 13-16 were 0.73, 0.74, and 0.72, respectively.

C. Performance with Bands 1–3,7–9, and 13–16 (10 Bands Only)

Bands 1–3, 7–9, and 13–16 outperformed the previous two categories with an accuracy of 78.03%. Figure 3(c) displays the confusion matrices for Bands 1–3, 7–9, and 13–16. The accuracy increased when these bands were combined with RGB, topographical features, and other features such as NDVI, NDBI, and NDWI. The landslide pixels had a recall of 0.83, compared to non-landslide images, which had a recall of 0.69. The false positive cases dropped to 54, compared to Bands 1–3 and 13-16, which had 89 false positive cases. This indicates reduced imbalance and improved accuracy for landslide and non-landslide pixels, compared to the previous two bands. The weighted average precision, recall, and F1-score for these bands were 0.78, 0.78, and 0.78, respectively.

D. Performance with All Bands (1–16)

When the full spectral range was used, the model's test accuracy improved to 79.47%. The test accuracy (0.79) and confusion matrix in Figure 3(d) demonstrate a more balanced classification between landslide and non-landslide cases, with recall values of 0.90 and 0.60, respectively. The landslide class achieved an F1-score of 0.85, while the non-landslide class achieved 0.68, reflecting a substantial improvement in predictive reliability across both classes. As depicted in Figure 2, weighted average precision, recall, and F1-score for these bands were 0.79, 0.79, and 0.79, respectively. This indicates that additional spectral information enables CNN to better classify terrain characteristics associated with landslides.

E. Comparative Analysis

A comparative bar chart of performance metrics, as shown in Figure 2, further illustrates these findings. Across all metrics—accuracy, precision, recall, and F1-score—the all-band configuration outperformed the limited-band configuration. This confirms that the inclusion of diverse spectral bands provides richer feature representations, enabling CNN to capture subtle variations in soil, vegetation, and surface conditions that are strongly associated with landslide prediction.

F. Discussion

The results highlight the importance of spectral diversity for landslide prediction models. While a limited band set (Bands 1–3) may capture basic surface reflectance properties, it fails to account for the complex interactions of vegetation cover, soil moisture, and geological conditions that are revealed in other spectral ranges. The improved performance with all bands (Bands 1–16) validates the use of multispectral data for robust landslide prediction. The CNN model was implemented using a limited dataset of 2,453 Landsat satellite images, comprising 1,558 landslide images and 875 non-landslide images.

Advanced techniques, such as data augmentation, were employed to increase the number of images, thereby enhancing accuracy. However, the model has some limitations, including the limited dataset and hyperparameter tuning. Collecting images from a wider array of satellites could further boost the number of satellite images, potentially yielding better results than those currently achieved. With additional epochs and appropriate hyperparameter tuning, the model's performance can be further improved.

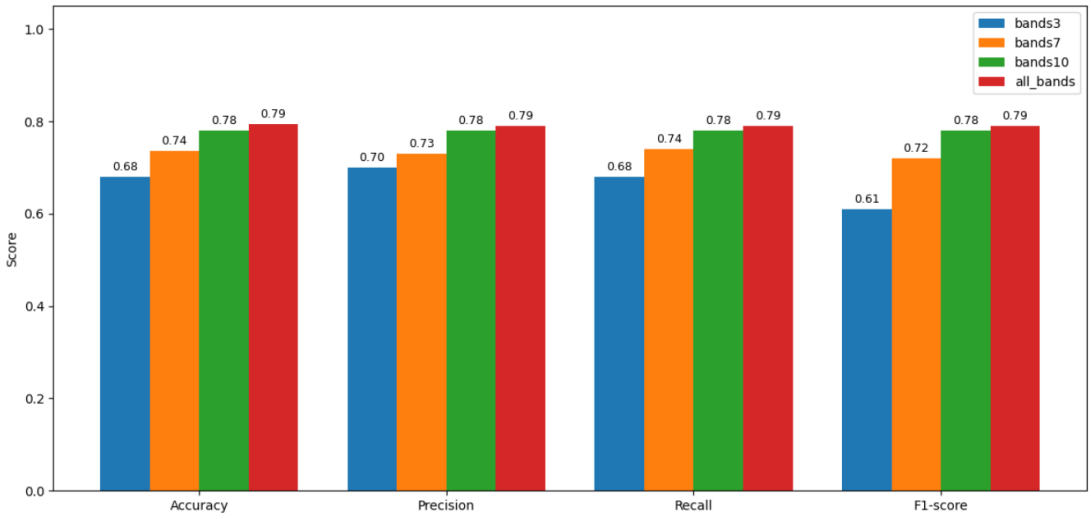

Fig. 2. Performance comparison with different numbers of band selection.

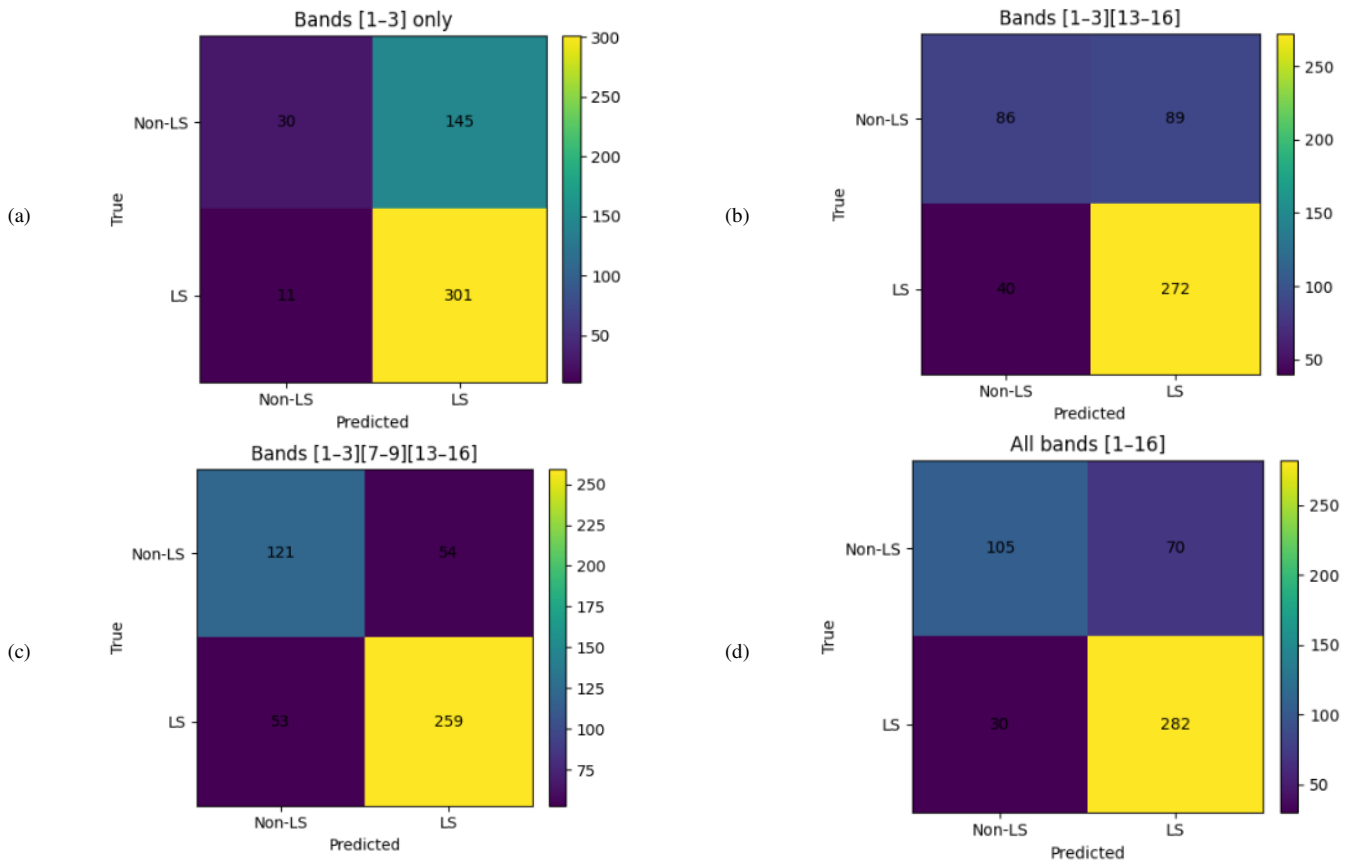

Fig. 3. Confusion matrices for models with different numbers of bands: (a) bands 1–3, (b) bands 1–3 and 13-16, (c) bands 1–3, 7–9, and 13–16, and (d) all bands (1–16).

IV. CONCLUSION

This study investigated the potential of deep learning models, specifically Convolutional Neural Networks (CNNs), for landslide prediction using multi-spectral remote sensing data and ancillary topographic variables. A dataset of 1558 landslide samples and 875 non-landslide samples was used. It comprised 64×64 pixel image patches extracted from 16 spectral bands along with indices such as NDVI, NDWI, NDBI, and terrain factors (slope, elevation, aspect, curvature). The proposed CNN architecture achieved a test accuracy of 79.47% with all 16 bands by considering all features, while the limited band subsets exhibited lower accuracy. With 3 bands, the landslide prediction accuracy was only 67.97%, which increased to 73.51% and 78.03% for 5 and 10 bands, respectively. This demonstrates that the landslide prediction accuracy increases with an increase in the number of bands. Additionally, a comparative analysis confirmed that combining all spectral and terrain features results in superior predictive performance. For future work, a larger dataset could be used to further improve prediction accuracy.

REFERENCES

[1] S. L. Ullo *et al.*, "Landslide Geohazard Assessment with Convolutional Neural Networks Using Sentinel-2 Imagery Data," in *2019 IEEE International Geoscience and Remote Sensing Symposium*, Yokohama, Japan, July 2019, pp. 9646–9649, https://doi.org/10.1109/IGARSS.2019.8898632.

[2] L. Zhu, G. Wang, F. Huang, Y. Li, W. Chen, and H. Hong, "Landslide Susceptibility Prediction Using Sparse Feature Extraction and Machine Learning Models Based on GIS and Remote Sensing," *IEEE Geoscience and Remote Sensing Letters*, vol. 19, pp. 1–5, 2022, https://doi.org/10.1109/LGRS.2021.3054029.

[3] K. V. Vishnu Vardhan, V. H. S. S. Kaushik, K. L. Sailaja, and P. R. Kumar, "Detection and Prediction of Landslide Vulnerability through Case Study using DInSAR Technique and U-Net Model," in *2023 5th International Conference on Smart Systems and Inventive Technology*, Tirunelveli, India, Jan. 2023, pp. 176–182, https://doi.org/10.1109/ICSSIT55814.2023.10061077.

[4] S. Senthil Pandi, P. Kumar, R. M. Suchindhar, P. Karupannan, "Hybrid Slide Sense: A Holistic Approach to Predicting Landslide Susceptibility via Deep Learning and Machine Learning," in *2024 International Conference on Emerging Technologies and Innovation for Sustainability*, Greater Noida, India, Dec. 2024, pp. 300–305, https://doi.org/10.1109/EmergIN63207.2024.10961733.

[5] A. Gobinath, P. Rajeswari, G. Yuvashree, K. Swastika, and K. A. Ishwarya, "A Comprehensive Hybrid CNN-LSTM Deep Learning Model for Accurate Landslide Prediction," in *2024 International BIT Conference*, Dhanbad, India, Dec. 2024, pp. 1–4, https://doi.org/10.1109/BITCON63716.2024.10985324.

[6] Y. J. Kumar *et al.*, "Developing Sustainable Solutions Using Technological Approaches for Disaster Management and Energy Access in Mountainous Ranges: A Case Study of Sera Village, India," in *2024 Fourth International Conference on Advances in Electrical, Computing, Communication and Sustainable Technologies*, Bhilai, India, Jan. 2024, pp. 1–6, https://doi.org/10.1109/ICAECT60202.2024.10469266.

[7] G. Kour and N. Rathour, "Landslide Detection and Mapping using Remote Sensing U-Net Model in Leh-Ladakh Region," in *7th International Conference on Contemporary Computing and Informatics*, Greater Noida, India, Sept. 2024, pp. 1044–1049, https://doi.org/10.1109/IC3I61595.2024.10829154.

[8] V. Acharya, A. Ghosh, I. Kang, T. Munasinghe, and K. C. Binita, "Landslide Likelihood Prediction Using Machine Learning Algorithms," in *2022 IEEE International Conference on Big Data*, Osaka, Japan, Dec. 2022, pp. 5395–5403, https://doi.org/10.1109/BigData55660.2022.10020433.

[9] Z. Zhao, T. Chen, J. Dou, G. Liu, and A. Plaza, "Landslide Susceptibility Mapping Considering Landslide Local-Global Features Based on CNN and Transformer," *IEEE Journal of Selected Topics in Applied Earth Observations and Remote Sensing*, vol. 17, pp. 7475–7489, 2024, https://doi.org/10.1109/JSTARS.2024.3379350.

[10] B. Sarada, P. Varsha, N. Sindhu, and M. Uma, "An Intuitive Approach with CNN Model for Landslide Prediction Using Satellite Imagery," in *2025 4th International Conference on Distributed Computing and Electrical Circuits and Electronics*, Ballari, India, Apr. 2025, pp. 1–8, https://doi.org/10.1109/ICDCECE65353.2025.11035499.

[11] V. Banupriya, V. G. Indhusri, S. Kaviya, J. Kiruthika, R. Soundarya, "Flood and Landslide Prediction and Risk Assessment System using Deep Learning with GSM-based Real Time Alerts," in *7th International Conference on Intelligent Sustainable Systems*, Tirunelveli, India, Mar. 2025, pp. 1542–1545, https://doi.org/10.1109/ICISS63372.2025.11076263.

[12] H. Yan, A. Khan, A. Jamil, B. Abdeldjalil, T. Saidani, and N. Y. Rebouh, "Deep Learning-Based Spatial Prediction of Landslide Risk in Coastal Areas Using GIS and Multicriteria Decision Making: A DeepLabV3+ Approach," *IEEE Journal of Selected Topics in Applied Earth Observations and Remote Sensing*, vol. 18, pp. 15222–15235, 2025, https://doi.org/10.1109/JSTARS.2025.3578822.

[13] Y. He *et al.*, "A Heterogeneous Ensemble Learning Method Combining Spectral, Terrain, and Texture Features for Landslide Mapping," *IEEE Journal of Selected Topics in Applied Earth Observations and Remote Sensing*, vol. 18, pp. 3746–3765, 2025, https://doi.org/10.1109/JSTARS.2025.3525633.

[14] G. B. Raj, M. K. Patan, A. K. Gupta, C. Lakshmi, D. Gopinath, A. S. Yadav, "A Novel Methodology to Predict Flood and Landslide Disasters using Learning Assisted Artificial Intelligence (AI) Logic," in *2025 International Conference on Electronics and Renewable Systems*, Tuticorin, India, Feb. 2025, pp. 1860–1867, https://doi.org/10.1109/ICEARS64219.2025.10940940.

[15] Y. Chen *et al.*, "Quantitative Hazard Prediction of Rainfall-Induced Shallow Landslides Considering Triggering and Predisposing Factors: A Case of Natural Terrain Landslides in Hong Kong," *IEEE Journal of Selected Topics in Applied Earth Observations and Remote Sensing*, vol. 18, pp. 13472–13488, 2025, https://doi.org/10.1109/JSTARS.2025.3570020.

[16] D. Anil and S. H. Manjula, "High-Precision Landslide Susceptibility Mapping Using CNN-LSTM-Attention Models," *Engineering, Technology & Applied Science Research*, vol. 15, no. 4, pp. 25486–25491, Aug. 2025, https://doi.org/10.48084/etasr.11505.

[17] "Earth Engine Data Catalog." Google Earth Engine, 2025, [Online]. Available: https://developers.google.com/earth-engine/datasets/catalog/.

[18] "Landslides Datasets." GPM IMERG, 2025, [Online]. Available: https://www.earthdata.nasa.gov/topics/human-dimensions/landslides/data-access-tools#toc-landslides-datasets.